Molecular Crystals and Liquid Crystals
Publication details, including instructions for authors and subscription information:
http://www.tandfonline.com/loi/gmcl16

Electric Effects in MBBA/PEBAB Mixtures

R. A. Kashnow [a] & H. S. Cole [a]
[a] General Electric Company Corporate Research and Development, Schenectady, New York, U.S.A.
Version of record first published: 21 Mar 2007.

To cite this article: R. A. Kashnow & H. S. Cole (1973): Electric Effects in MBBA/PEBAB Mixtures, Molecular Crystals and Liquid Crystals, 23:3-4, 329-342

To link to this article: http://dx.doi.org/10.1080/15421407308083380

Molecular Crystals and Liquid Crystals. 1973. Vol. 23, pp. 329–342

Printed in Great Britain

Electric Effects in MBBA/PEBAB Mixtures†

R. A. KASHNOW and H. S. COLE

General Electric Company
Corporate Research and Development
Schenectady, New York
U.S.A.

Received October 31, 1972

Abstract—The principal low-frequency dielectric constants have been measured for the binary mixture $(\text{MBBA})_{1-x}$ $(\text{PEBAB})_x$, for mole fractions up to $x=0.21$. In this range $\Delta\epsilon$ varies linearly with x changing sign at $x \simeq 0.02$, and a room-temperature mesophase is preserved. Eor $\Delta\epsilon < 0$, we consider the effect of varying $/\Delta\epsilon/$ on the threshold condition for instability in the presence of low- and high-frequency fields. For $\Delta\epsilon > 0$, we study the Freedericksz transition, using an approximation which leads to a closed-form expression for the variation of phase retardation with voltage. Electrohydrodynamic instabilities are observed in the positive regime.

1. Introduction

In the study of a variety of electric field effects in liquid crystals, as well as in their application to electrooptic devices, the low-frequency dielectric anisotropy is a parameter of primary importance. Whereas the principal dielectric constants are sensitive to (sometimes subtle) details of molecular structure, they are amenable to continuous variation in binary mixtures of nematogenics. In this paper, we report some studies of electric field effects in mixtures of two Schiff's base nematics: *N*-(*p*-methoxybenzylidene)-*p*-butylaniline (MBBA) and *p*-[(*p*-ethoxybenzylidene) amino] benzonitrile (PEBAB). MBBA is nematic in the range 20 to 47 °C and exhibits a small negative dielectric anisotropy[1] (NDA) $\Delta\epsilon \equiv \epsilon_p - \epsilon_t \simeq -0.5$, where the subscripts denote components parallel to and transverse to the long molecular axis. PEBAB, nematic from 105 to 127 °C, has a strongly positive dielectric anisotropy[2] (PDA) $\Delta\epsilon \gtrsim 20$, due largely to

† Presented (as paper no. 82) at the Fourth International Liquid Crystal Conference, Kent, Ohio, 1972.

the presence of a terminal cyano group. We report, below, measurements of ϵ_p and ϵ_t for the mixture $(MBBA)_{1-x}$ $(PEBAB)_x$, where the mole fraction, x, has been varied from 0 to 0.21. With these mixtures, we are able to conveniently study electrooptic effects in both regimes, $\Delta\epsilon < 0$ and $\Delta\epsilon > 0$. Specifically, we discuss the following:

i) for $\Delta\epsilon < 0$, the dependence on $|\Delta\epsilon|$ of the instability threshold condition for the special case of simultaneous application of low- and high-frequency electric fields;[3,4]

ii) for $\Delta\epsilon > 0$, the dependence on voltage and $\Delta\epsilon$ of the phase retardation in a Freedericksz transition[5] from planar boundary conditions;

iii) some electrohydrodynamic instabilities for $\Delta\epsilon > 0$.

2. Measurements of Dielectric Constants

The principal dielectric constants, ϵ_p and ϵ_t were measured for eight samples of varying concentration of PEBAB in MBBA. We restricted ourselves to the range $0 < x < 0.21$, where x is the mole fraction of PEBAB, in order to preserve the room-temperature range of the mesophase (see Fig. 1). The dielectric constants were inferred from capacitance measurements at 1 kHz at 23 °C on samples which were contained in sealed, parallel-plate capacitors, with tin-oxide-coated glass substrates. Parasitic capacitances and geometrical factors were determined by measuring cell capacitances both empty and with chlorobenzene. A 13 kGauss magnetic field was sufficient to align the nematic director predominantly parallel or perpendicular to the electrodes. The samples used had resistivities of order 10^{10} ohm-cm; the conductivity ratio σ_p/σ_t was 1.50 for small x and rose slightly for the highest PEBAB concentrations.

In Fig. 2, ϵ_p and ϵ_t are plotted as a function of x. Figure 3 shows the dielectric anisotropy, $\Delta\epsilon \equiv \epsilon_p - \epsilon_t$ for these data. The point of dielectric isotropy occurs near $x = 0.02$. Within our experimental error, the dielectric constants increase linearly with x above this point, and their difference, $\Delta\epsilon$, is approximately linear with x over the entire range measured (the solid line in Fig. 3 results from a least-squares-fit and has a slope of 0.31 for the units shown).

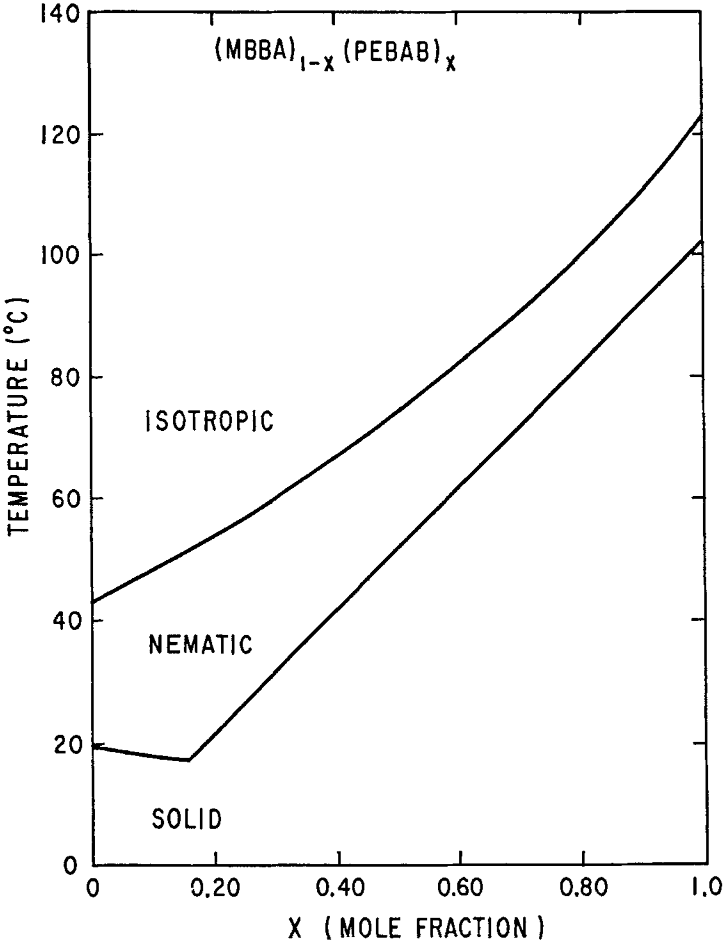

Figure 1. Phase diagram for $(MBBA)_{1-x}$ $(PEBAB)_x$.

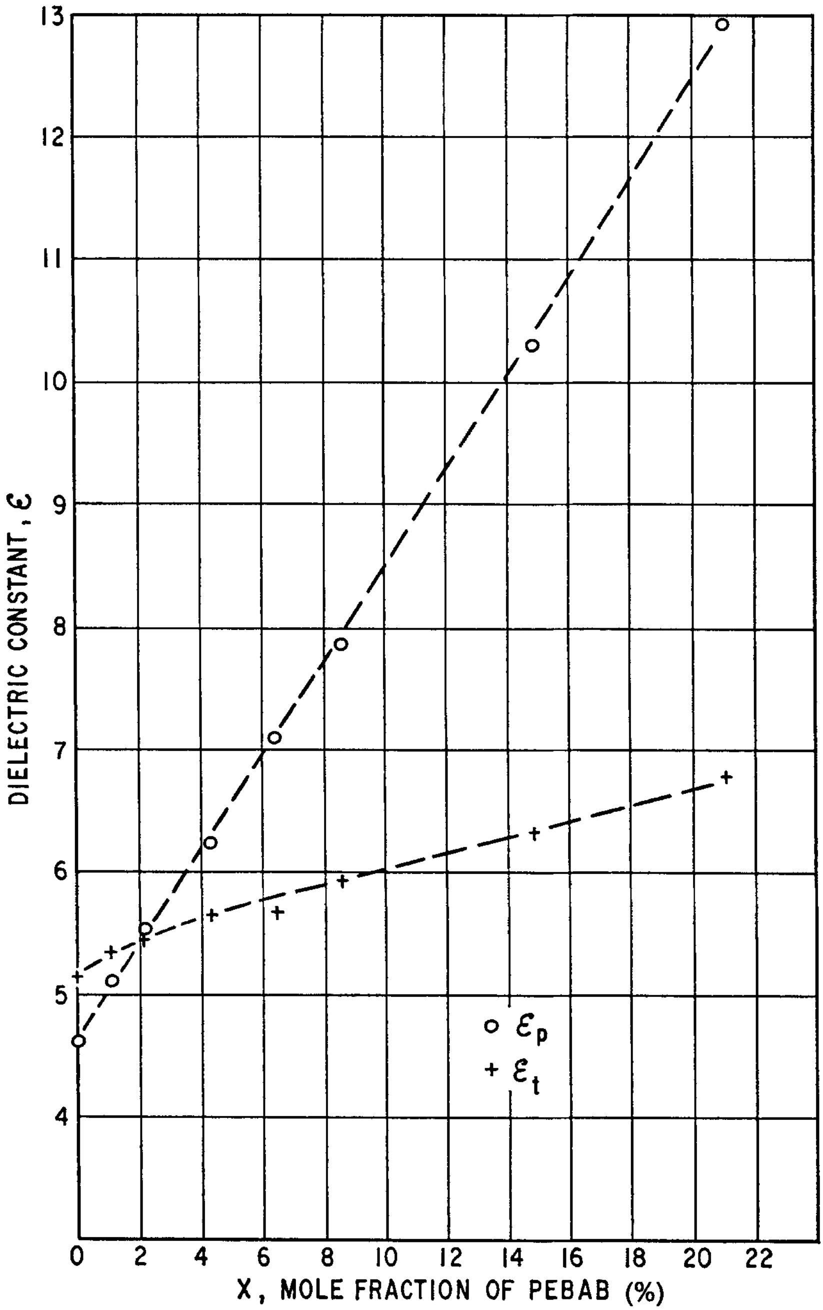

Figure 2. The principal dielectric constants, ϵ_p and ϵ_t, of nematic $(MBBA)_{1-x}$ $(PEBAB)_x$, measured at 1000 Hz and room temperature.

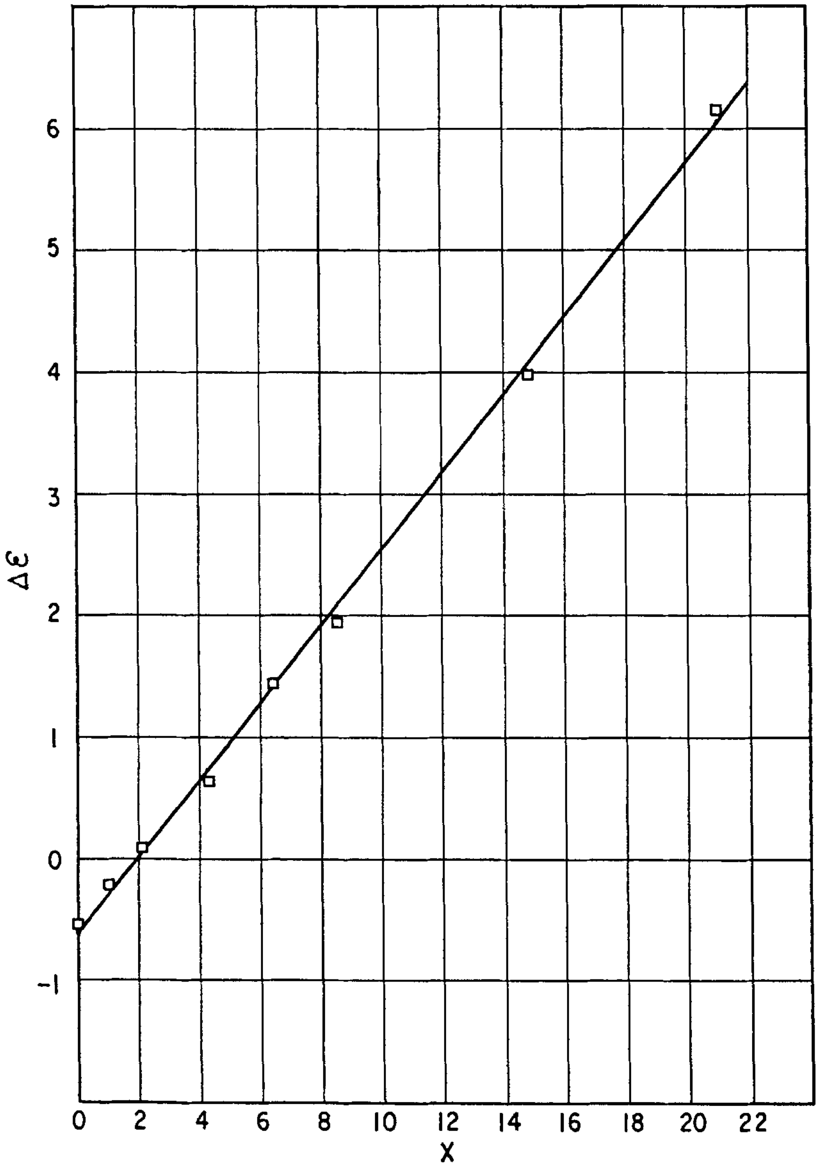

Figure 3. The dielectric anisotropy, $\Delta\epsilon$, *vs.* x, the mole fraction of PEBAB in nematic mixtures of the form $(MBBA)_{1-x}$ $PEBAB_x$; measured at room temperature and 1000 Hz. The solid line is a least-squares-fit to the data.

3. Two-Frequency Threshold Measurements

Dynamic scattering displays (which use nematics of NDA) can be multiplexed by an addressing technique which employs the simultaneous application of low- and high-frequency ac signals.[3,4] If sinusoidal waveforms with rms voltages $V_1(f_1)$ and $V_2(f_2)$ are applied simultaneously, where $f_1 \ll f_c < f_2$ and f_c is the cutoff frequency separating the conduction and dielectric regimes,[6] the threshold condition for domain formation can be written as

$$V_1^2 = V_H^2 + \gamma V_2^2. \tag{1}$$

V_H is the Helfrich threshold[7] and

$$\gamma = -\Delta\epsilon(\epsilon_t/\epsilon_p)\left\{\frac{\kappa_1}{\eta_1}\epsilon_p\left(\frac{\epsilon_t}{\epsilon_p} - \frac{\sigma_t}{\sigma_p}\right) + \Delta\epsilon\frac{\sigma_t}{\sigma_p}\right\}^{-1} \tag{2}$$

The shear-torque and viscosity coefficients κ_1 and η_1 were measured by Gahwiller[8] for MBBA; the ratio is $\kappa_1/\eta_1 = 0.75$.

In Fig. 4, we have plotted V_1^2 vs. V_2^2 (Eq. (1)) for three samples, containing respectively the molar fractions $x = 0$, $x = 0.008$, and $x = 0.016$ of PEBAB in MBBA. In each case, the data were taken for frequencies far from f_c, although corrections to Eq. (1) can be

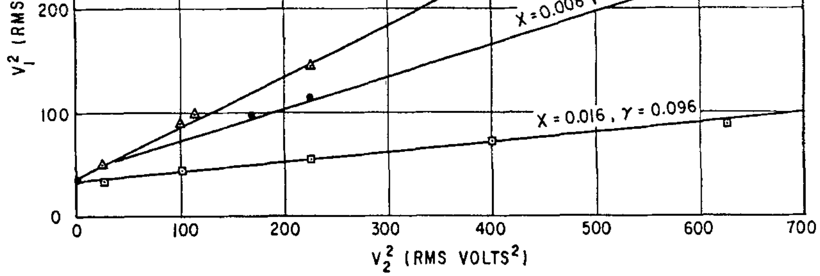

Figure 4. Instability threshold data for simultaneous application of voltages at low- (V_1) and high- (V_2) frequencies to nematics with $\Delta\epsilon < 0$. x denotes the mole fraction of PEBAB added to MBBA. γ is the slope (see text).

made when the inequality $f_1 \ll f_c$ does not obtain.[4,9] The solid line for the $x = 0$ (pure MBBA) sample is calculated from Eq. (2) and agrees well with the experiment, as mentioned above. For the samples containing some PEBAB, however, Eq. (2) predicts values of γ which are lower than the experimental values if the value of κ_1/η_1 for MBBA is assumed unchanged. Therefore, for the $x = 0.008$ and $x = 0.016$ samples, the solid lines shown in Fig. 4 were determined by least-squares-fit to the data. The values of γ are 0.31 and 0.096, respectively, and, using the measured dielectric constants and conductivities for these samples, correspond to values of κ_1/η_1 of 0.55 and 0.43 respectively.

The dependence of γ on $\Delta\epsilon$ is of technical importance in the selection of an appropriate nematic for application of the two-frequency addressing technique. For example, we have found $\gamma = 0.1$ for Merck IV,[10] for which $\Delta\epsilon = -0.2$. Such a low value of γ requires relatively large high-frequency voltages to be employed, and this renders the addressing technique impractical. Satisfactory values of γ (between 0.5 and 0.6) are found[9] for MBBA and MBBA/EBBA mixtures[11] for which $|\Delta\epsilon| \gtrsim 0.5$. Similarly, $\gamma \simeq 0.7$ for the nematic mixture EK11643.[12]

4. Voltage-Dependence of the Phase Retardation in a Freedericksz Transition

4.1. Theory

With reference to Fig. 5, we consider a thin planar nematic sample with $\Delta\epsilon > 0$. The boundary conditions on the nematic director are $\mathbf{n}(0) = \mathbf{n}(d) = \mathbf{x}$. An ac electric field is applied parallel to $\mathbf{z}$, so that $\mathbf{n}(z)$ makes an angle $\theta(z)$ with $\mathbf{z}$. Although this configuration has been treated before for both the magnetic-[13] and electric-[14]field cases, our purpose here is to express the voltage-dependence of the phase retardation in a closed form which is convenient for analysis, particularly for device purposes where this, or formally similar electrooptic effects are used.

If we restrict ourselves to voltages significantly above the threshold for the Freedericksz transition, we can expect the coherence length ξ to be small compared to the sample thickness. In this limit we

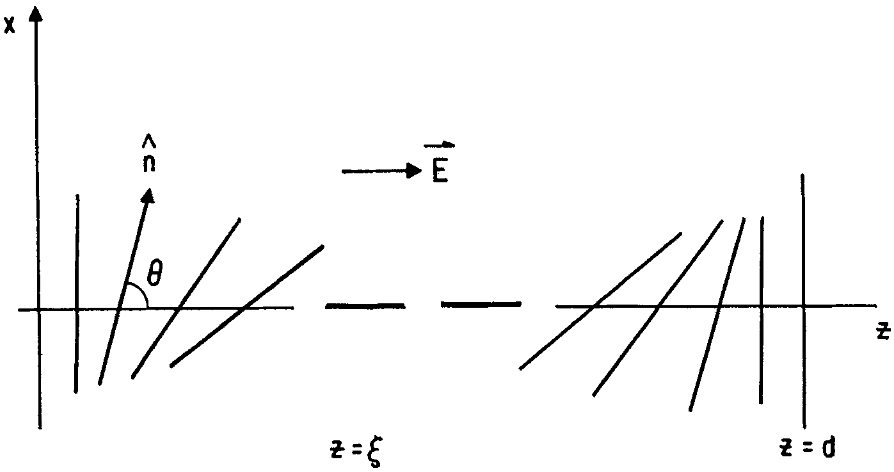

Figure 5. Distribution of the nematic director in a Freedericksz transition from planar boundary conditions for the case of $\Delta\epsilon > 0$ and high-fields.

can use the electric-field analogue of de Gennes' expression[15] for $\theta(z)$ developed for a semi-infinite medium:

$$\tan(\theta(z)/2) = \exp(-z/\xi) \tag{3}$$

where the coherence length is

$$\xi = (K/\Delta\epsilon)^{1/2} E^{-1} \tag{4}$$

and K is to be regarded as an average elastic constant for bend and splay deformations.

Next, consider the phase differences dδ between ordinary and extraordinary rays of wavelength λ after traversing an infinitesimally thin layer dz of a uniaxial birefringent medium. If Θ is the angle of incidence and ψ the angle between the optic axis and the (average) refracted ray direction in the medium,[16]

$$\mathrm{d}\delta = 2\pi\Delta n\,\mathrm{d}z \sin^2\psi/\lambda \cos\Theta. \tag{5}$$

Equation (5) is approximate in that it assumes the birefringence Δn to be very small compared to n_o and n_e, the refractive indices for ordinary and extraordinary rays, respectively.

For normal incidence ($\Theta = 0$), $\psi = \theta$ (as in Fig. 5 and Eq. (3)). The total phase retardation for a sample of thickness d is then

$$\delta = (4\pi\Delta n/\lambda)\int_{z=0}^{d/2} \sin^2\theta(z)\,\mathrm{d}z. \tag{6}$$

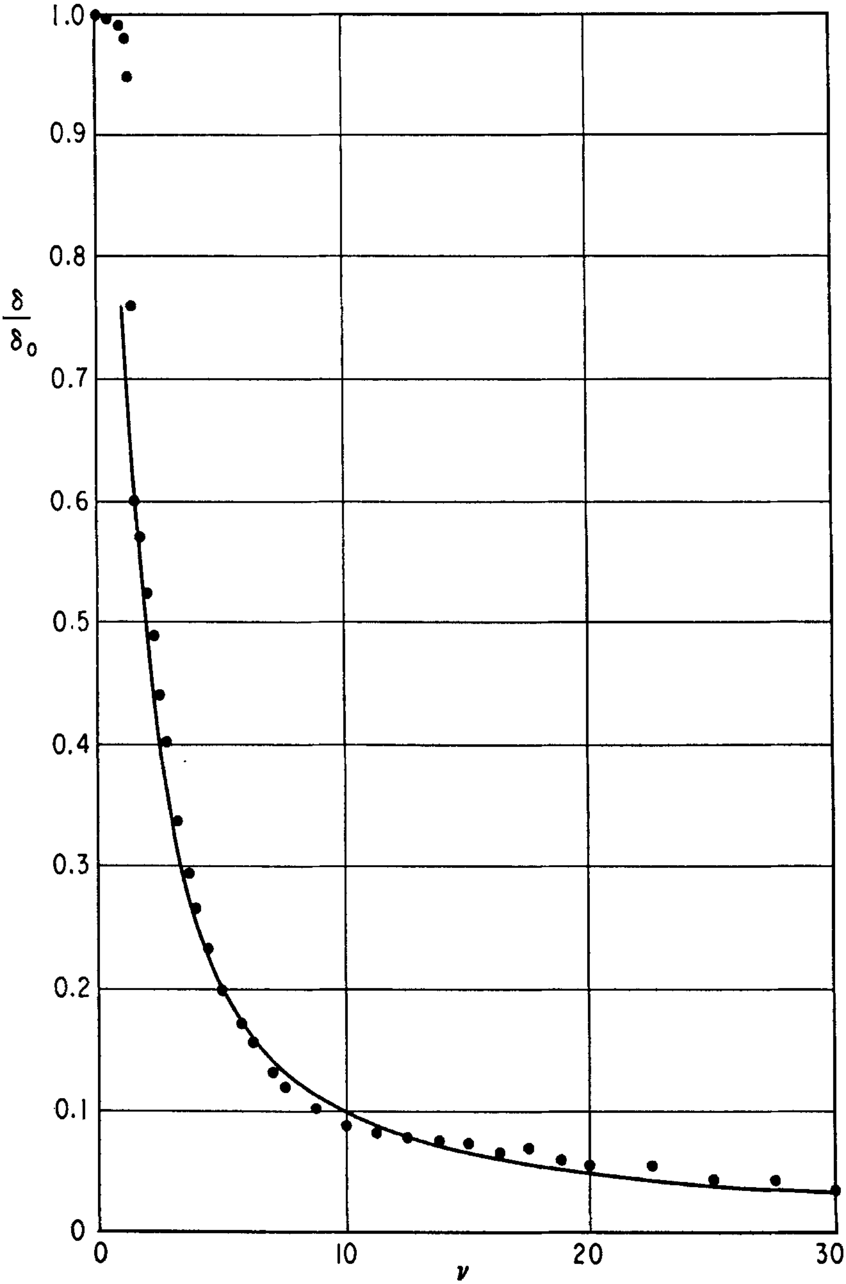

Figure 6. Normalized phase retardation *vs.* reduced voltage for the transition shown in Fig. 4. The points are experimental for a sample with 0.21 mole fraction of PEBAB in MBBA. The solid line is calculated from Eq. (8).

To evaluate this integral, we express $\sin\theta$ in terms of $\tan\theta/2$ and use Eq. (3):

$$\begin{aligned}\delta &= (4\pi\Delta n/\lambda)\left\{d/2 - \int_0^{d/2}\left[\frac{1-\exp(-2z/\xi)}{1+\exp(2z/\xi)}\right]^2 \mathrm{d}z\right\}\\ &= (4\pi\Delta n/\lambda)\left\{d/2 - \int_0^{d/2}\tanh^2(z/\xi)\,\mathrm{d}z\right\}\\ &= (4\pi\Delta n/\lambda)\left(\xi\tanh\frac{d}{2\xi}\right).\end{aligned} \tag{7}$$

Using (4), we can rewrite,

$$\delta = \delta_0\,\nu^{-1}\tanh\nu, \tag{8}$$

where δ_0 is the zero-field retardation,

$$\delta_0 = 2\pi\Delta n\, d/\lambda \tag{9}$$

and ν is a reduced voltage,

$$\nu \equiv Ed/2(K/\Delta\epsilon)^{1/2} = V/2(K/\Delta\epsilon)^{1/2}. \tag{10}$$

The function $\delta/\delta_0 = (\tanh\nu)\nu^{-1}$ is shown as a solid line in Fig. 6. Note that the curve is not shown for small values of ν, where it does not exhibit the abrupt threshold of the Freedericksz transition, but rather approaches unity continuously as $\nu \rightarrow 0$, exhibiting a point of inflection at $\nu = 1$. The agreement with experiment is quite good for larger values of ν, however; the comparison is discussed below.

4.2. Experiment

The phase retardations of several samples, of varying amounts of PEBAB in MBBA, were measured as a function of applied voltage. The measurements were made on a Zeiss polarizing microscope using the Senarmont technique[17] at $\lambda = 546$ (± 2) nm. Such data can be exhibited in the form δ/δ_0 vs. V, but a comparison with Eq. (8) requires a reconciliation of the quantity $(K/\Delta\epsilon)^{1/2}$.

The normalization is achieved by fitting the data for a particular sample to the curve at one point. For example, the data points in Fig. 6, for a $(\text{MBBA})_{1-x}$ $(\text{PEBAB})_x$ sample with $x = 0.21$ were fit by identifying the voltage ($V = 3.0$ vrms) at which $\delta/\delta_0 = 0.1$ with the value $\nu = 10$, for which the function $\tanh\nu/\nu = 0.1$. Equation (10) then gives $(K/\Delta\epsilon)^{1/2} = 0.175$ in mks units. Taking $\Delta\epsilon = 6.14$, we find $K = 1.7 \times 10^{-7}$ dyne. The data for samples with $x = 0.053$ and $x = 0.11$ could be fit to Eq. (8) using the same value of K and the measured values of $\Delta\epsilon$, namely, 2.60 and 1.0, respectively.

4.3. Discussion

The analysis described above is convenient for the description of electrooptic effects which involve Freedericksz transitions. For example, consider a planar nematic layer of PDA, oriented between crossed polarizers so that the optic axis in the quiescent state makes an angle of 45 degrees with the vibration directions of the polarizers. The layer thickness, d, can be adjusted such that, in Eq. (9), $\delta_0 = \pi/4 + n\pi$ (where n is an integer); for this condition, maximum transmission through the crossed pols obtains. For applied voltages above threshold, δ then varies according to (8), and the transmission through the pols is modulated. Figure 6 shows the extent to which the alignment of the layer is incomplete, even at voltages far above threshold. The residual phase retardation (due to the finite coherence length at the boundaries) prevents the achievement of maximum darkness (through the pols) for moderate voltages. By contrast, this problem is avoided in devices which utilize the alignment of a twisted nematic structure[10] provided the polarization direction of incident light does not make an angle different from 0 or $\pi/2$ with the residual boundary layers.

The variable phase retardation in a Freedericksz transition can be used, however, to achieve control of Newton's colors through the polarizers. Recently, several authors have described the performance of such devices based on the deformation, in a high-frequency electric field, of a homeotropic layer of NDA nematic.[10–21] The analysis leading to (8) can be applied with a slight modification, with the result that

$$\delta/\delta_0 = 1 - \tanh \nu/\nu. \tag{11}$$

5. Electrohydrodynamic Instabilities for $\Delta\varepsilon > 0$

Finally, some mention must be made of electrohydrodynamic instabilities in the PDA regime.[22–25] Recently, De Jeu *et al.*[25] showed that the threshold voltage for apparent dielectric alignment in certain PDA nematics changes continuously into an instability threshold above the dielectric relaxation frequency at which $\Delta\epsilon$ changes sign. This suggests that the hydrodynamics may be important at the lower frequencies as well (i.e. for $\Delta\epsilon > 0$).[26]

In our experiments with PDA PEBAB/MBBA mixtures, we have observed a variety of instability domain patterns (see Figs. 7 and 8) at ac frequencies, but always at voltages greater than the threshold for realignment (starting with parallel boundary conditions). Our preliminary observations have been that the instability threshold increases with field frequency, but we have not observed a diverging frequency dependence (for the maximum frequencies and voltages

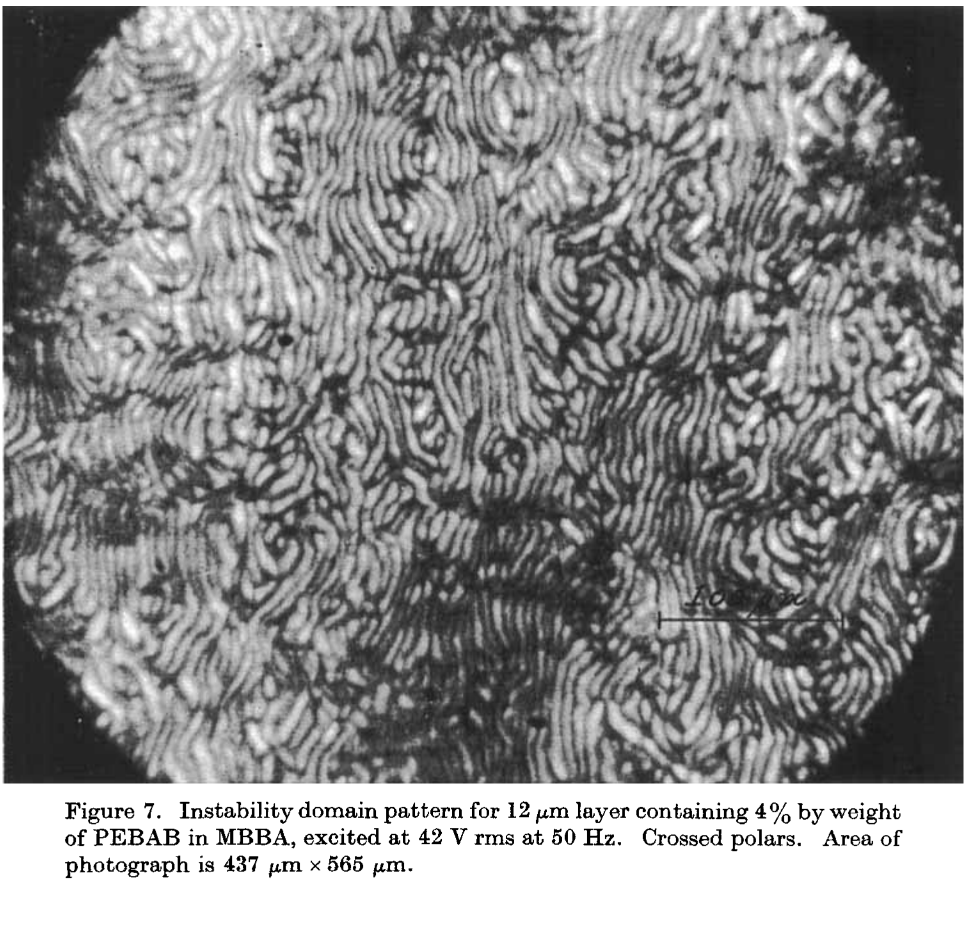

Figure 7. Instability domain pattern for 12 μm layer containing 4% by weight of PEBAB in MBBA, excited at 42 V rms at 50 Hz. Crossed polars. Area of photograph is 437 μm $\times$ 565 μm.

we can attain before breakdown) such as obtains in the conduction regime[6] of NDA materials. For example, for a 12 μm layer of 4% by weight of PEBAB in MBBA, V_{th} increases from about 37 vrms at 100 Hz to 79 vrms at 400 Hz to 114 vrms at 800 Hz. We have also noted that the instabilities in this high-field regime are not sensitive to the magnitude of $\Delta\epsilon$; moreover, the threshold voltage is not independent of sample thickness in the range of 6 to 25 μm. The flow patterns which underly these instabilities appear more complicated than those in the Williams' stripe regime; the associated light scattering (nearly totally depolarized) is weak and confined to small angles in the forward direction, presumably because the

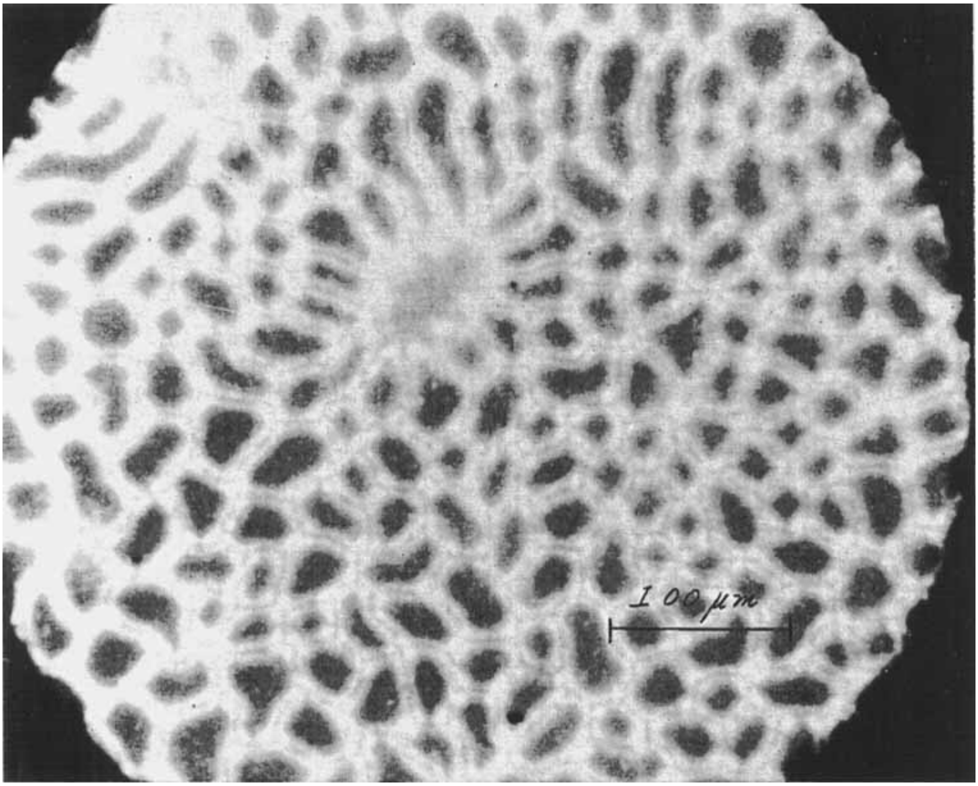

Figure 8. Instability domain pattern for 6 μm layer containing 14% by weight of PEBAB in MBBA, excited at 50 V rms at 40 Hz. Crossed polars. Area of photograph is 437 μm × 565 μm.

nematic director remains predominantly parallel to the applied field direction (i.e. the sample normal).

Acknowledgements

We acknowledge helpful conversations with J. E. Bigelow and P. G. de Gennes.

REFERENCES

1. Diguet, D., Rondelez, F. and Durand, G., *C. R. Acad. Sc. Paris* **271,** 954 (1970).
2. Schadt, M., *J. Chem. Phys.* **56,** 1494 (1972).
3. Stein, C. R. and Kashnow, R. A., *Appl. Phys. Letters* **19,** 343 (1971).
4. Wild, P. J. and Nehring, J., *Appl. Phys. Letters* **19,** 335 (1971).
5. Freedericksz, V. and Zolina, V., *Trans. Faraday Soc.* **29,** 919 (1933).
6. Orsay Liquid Crystal Group, *Phys. Rev. Letters* **25,** 1642 (1970).
7. Helfrich, W., *J. Chem. Phys.* **51,** 2755 (1969).
8. Gahwiller, Ch., *Phys. Letters* **36a,** 311 (1971).
9. Stein, C. R. and Kashnow, R. A., Society for Information Display International Symposium, San Francisco, 1972.
10. E. Merck Company, Darmstadt, Germany.
11. " EBBA denotes *N*-(*p*-ethoxybenzylidene)-*p*-butylaniline.
12. Eastman Kodak Company, Rochester, New York.
13. Saupe, A., *Z. Naturforschg.* **15a,** 815 (1960).
14. Gruler, H. and Meier, G., *Mol. Cryst. and Liq. Cryst.* **16,** 299 (1972).
15. de Gennes, P. G., *Mol. Cryst. and Liq. Cryst.* **7,** 325 (1969).
16. Born, M. and Wolf, E., *Principles of Optics*, Pergamon Press, Oxford, 1965, p. 699.
17. Hartshorne, N. H. and Stuart, A., *Crystals and the Polarising Microscope*, American Elsevier, New York, 1970, p. 309.
18. Schadt, M. and Helfrich, W., *Appl. Phys. Letters* **18,** 127 (1971).
19. Schiekel, M. F. and Fahrenschon, K., *Appl. Phys. Letters* **19,** 391 (1971).
20. Soref, R. A. and Rafuse, M. J., *J. Appl. Phys.* **43,** 2029 (1972).
21. Kahn, F. J., *Appl. Phys. Letters* **20,** 199 (1972).
22. Dubois-Violette, E., de Gennes, P. G. and Parodi, O., *J. de Phys.* **32,** 305 (1971).
23. Gruler, H. and Meier, G., *Mol. Cryst. and Liq. Cryst.* **12,** 289 (1971).
24. De Jeu, W. H., Gerritsma, C. J. and Van Boxtel, A. M., *Phys. Letters* **34A,** 203 (1971).
25. De Jeu, W. H., Gerritsma, C. J., Van Zanten, P. and Goossens, W. J. A., *Phys. Letters* **39A,** 355 (1972).
26. Elastic constants deduced from a dielectric analysis of electric-field experiments may be in error due to neglect of the hydrodynamics. Comparison with magnetic field experiments on the same samples appears necessary. W. H. De Jeu, private communication. See, also, Ref. 14.